On the future evolution of heatwaves in French cities and associated rural areas: Insights from a convection-permitting model

Y. Michau, A. Lemonsu, P. Lucas-Picher, M. Schneider, Cécile Caillaud

On the future evolution of heatwaves in French cities and associated rural areas: insights from a Convection-Permitting Model

MICHAU Y. [1], LEMONSU A. [1], LUCAS-PICHER P. [1,2], SCHNEIDER M.[3], CAILLAUD C. [1]
[1] Centre National de Recherches Météorologiques (CNRM), Université de Toulouse, Météo-France, CNRS, Toulouse, France
[2] Département des sciences de la Terre et de l'atmosphère, Université du Québec à Montréal, Montréal, Canada
[3] Météo-France, Toulouse, France

Corresponding author: Yohanna MICHAU (yohanna.michau@meteo.fr)
ORCID:
Yohanna MICHAU (0000-0003-0781-9783)
Aude LEMONSU (0000-0001-8894-0088)
Philippe LUCAS-PICHER (0000-0001-8707-7745)
Michel SCHNEIDER (/)
Cécile CAILLAUD (0000-0003-2317-4129)

Abstract.
Urban areas are currently vulnerable to the effects of extreme weather events. Climate change is expected to increase such events, including heatwaves, on which we are focusing on. Our aim is to quantify how heatwave exposure will evolve with climate change and its impact on populations. We take advantage of the convection-permitting scale of CNRM-AROME (2.5-km) coupled with the urban canopy model TEB, to capture urban effects (in particular urban heat island, UHI) and their interactions with regional processes. The climate simulations cover an extended area of France for historical (1986-2005) and future (2080-2099) periods using the RCP8.5 emission scenario. The heatwave indicator (based on Ouzeau et al., 2016) is applied separately to assess the respective exposure of urban and associated rural areas. CNRM-AROME projects a strong shift in the minimum and maximum temperature distribution to warmer values in the future, especially in rural areas. Related to the stronger rural temperature increase, the model projects a diurnal and nocturnal UHI reduction. Nevertheless, heatwaves maximum intensity, duration and frequency are projected to increase in both urban and rural areas with climatic and geographical disparities. The results will soon be extended to a multi-model approach in the framework of CORDEX FPS URB-RCC.

Keywords.
Convection-Permitting Model, CNRM-AROME, Urban Climate, TEB, Climate change, Heatwaves

Highlights.

- The CPRCM AROME simulates the past heatwaves in a realistic way, both in terms of frequency and duration.
- Climate change is expected to lead to a strong shift towards warmer values and could exacerbate local climatic and geographical disparities.
- The nocturnal and diurnal UHI under heatwave conditions are expected to decrease by the end of the century in the 14 cities of metropolitan France.
- Urban and associated rural areas could be affected by an increase in the heatwaves duration, intensity and frequency, especially along the Atlantic and Mediterranean coasts.
- The countryside could become highly vulnerable to climate change due to changes in physical processes in the natural environment.

1. INTRODUCTION

The IPCC Fifth Assessment Report (IPCC AR5, 2014) unequivocally confirms the human impact on the climate system, causing an increase in global temperatures since the 1950s and consequent long-lasting changes in climate components and ecosystems. In European land areas, the average temperature has rapidly increased based on observations from 1970 to 2019 and will continue to rise under all assessed emission scenarios, at a rate surpassing global mean temperature changes (IPCC AR6, 2022). Since 1960, an increase was observed in the magnitude and frequency of the hottest extremes (IPCC AR6, 2022) that are projected to continue increasing in the coming decades (Russo et al., 2015). This increase is modulated with several climate conditions, such as anthropogenic forcing (Diffenbaugh et al., 2005), soil moisture (Fischer et al., 2007; Seneviratne et al., 2010), and the water surface temperature of the ocean (Schubert et al., 2016; Qasmi et al., 2021). According to the scientific community, a summer as hot as 2003 will likely become common in the future (Schär et al., 2004; Stott et al., 2004; Beniston, 2004; Christidis et al., 2015), resulting in health-related impacts, among others. For instance, during the infamous 2003 heatwave (HW, Fink et al., 2004), an excess of mortality in European cities was partially attributed to extreme heat (Robine et al., 2008), amplified locally by the Urban Heat Island (UHI) effect, such as in Paris, France (Laaidi et al., 2012). More recently, the extreme temperatures and dry conditions that hit European cities in the summer of 2022 had catastrophic impacts on human health and well-being, agriculture, food supply, energy prices and demand, and the natural ecosystem (Copernicus Climate Change Service, 2022).

The impacts of natural hazards are particularly significant in urban areas (Fallmann et al., 2015) due to the high population density and proximity assets (United Nations, Department of Economic and Social Affairs, 2019). Therefore, providing reliable information on climate change at the regional or urban scale is a major challenge for the scientific community to conduct vulnerability, impact, and adaptation studies. To achieve this, relevant climate indicators and methodologies specific to the type of extremes have to be evaluated, such as HW, which is the focus of this study. This will help the development of effective adaptation strategies and enhance the resilience against the impacts of climate change.

The World Meteorological Organization (WMO, 2022) defines a HW as a period of statistically unusual hot weather persisting for a number of days and nights. However, there is no consensus in the literature on the objective methodology and reliable thresholds for characterizing and reporting an HW (Suli et al., 2023). As mentioned for instance by Perkins & Alexander (2013) and Schoetter et al. (2015), it depends mainly on the context in which the study is performed (human health, electricity supply, transport, agriculture…).

Absolute thresholds are a useful tool for assessing the vulnerability and potential adaptation strategies of future HW. For example, biometeorological indices that refer to physiological limits of the population, such as the human capacity to recover from daytime heat by sleeping, have been applied in the framework of the French research project EPICEA (French acronym for *pluridisciplinary study of the impacts of climate change at the scale of Paris region*) by Lemonsu et al. (2013). These corresponding thresholds have been used in recent studies, in particular within the framework of the VURCA project (French acronym for *vulnerability of cities to future heatwaves and adaptation strategies)* by Lemonsu et al. (2014), and are also used in Daniel et al. (2018) or Viguié et al. (2020). These absolute thresholds are based on historical daily minimum and maximum temperature (TN/TX) by county, using excess mortality dataset collected by the Institute for Public Health Surveillance (InVS). Absolute thresholds are also appropriate for evaluating energy demand or mitigation temperatures strategies in buildings in the context of climate change. For instance, Baniassadi et al.

(2018) used the discomfort index (*i.e.*, indoor temperature > 26 °C) to evaluate indoor thermal conditions in warmer climates.

In addition, such thresholds have been used to analyze extreme heat events in weather monitoring. In the early years of development, the national operational warning system for extreme heat events in France was based on three absolute thresholds on daily mean temperature (TM), adjusted to clearly identified baseline events (*e.g.*, the HW events of 1947, 1976, 1983, 1994 and 2003). However, the HW detection method was improved in the last decade by using quantile thresholds, which allow for detection in varying climatic and geographical contexts (such as in coastal or mountainous areas), as described in Ouzeau et al. (2016). Most climate studies currently define extreme heat events by exceeding a quantile threshold, using the temperature distribution over a reference period (Machard et al., 2020). For instance, HWs are defined based on a single quantile threshold (*e.g.*, Fischer & Schär, 2010; D'Ippoliti et al., 2010; Perkins & Alexander, 2013; Russo et al., 2014, 2015), or on multiple quantile thresholds (*e.g.*, Ouzeau et al., 2016). These quantiles refer to the high extremes of the temperature distribution, as defined by the WMO. Quantile thresholds are primarily used to project the evolution of extreme heat events, including baseline events such as the hot and dry 2003 European summer in Fischer & Schär (2010), in the context of climate change. In Fischer & Schär (2010), for example, the 90th percentile threshold applied on daily maximum temperatures (TX) is used to characterize the meteorological and climatic aspects of extended hot episodes, including HW characteristics such as maximum duration, frequency, amplitude, and so on.

To study the vulnerability, impact, and adaptation of urban areas to climate change, advanced tools that consider the 3-D structures of cities, the complex interactions between global, regional, and local processes, and potential changes in urban areas (such as demographic trends and urban sprawl) and the urban climate (such as relevant climate projections) should be used. In recent years, convection-permitting regional climate models (CPRCM) with a horizontal resolution of less than 4 km (Kendon et al., 2021) have shown significant added value compared to coarser climate models (Soares et al., 2022). CPRCM could be coupled with dedicated urban canopy models to simulate urban areas for a range of urban-oriented studies (such as assessing day- and night-time urban heat islands in Keat et al., 2021; evaluating outdoor and indoor overheating in Shu et al., 2021; and simulating local atmospheric conditions and urban heat islands in Lemonsu et al., 2023). Such optimized models are increasingly used to evaluate the effectiveness of heat stress mitigation strategies and assess the effects of urbanization and climate change in urban areas (Argüeso et al., 2013; Keat et al., 2021).

In this study, we take advantage of the original configuration of Lemonsu et al. (2023) and Michau et al. (2023), based on a CPRCM coupled with a specific urban canopy model, to investigate the vulnerability of urban and rural areas to climate change. In Section 2, we present the numerical models used for our analysis, the selection of the cities, and the indicators and methodology implemented to assess the vulnerability of urban and rural areas to climate change. Section 3 is devoted to evaluating the ability of the CNRM-AROME CPRCM to simulate extreme heat events and to project the evolution of these events using the RCP8.5 scenario, which is the higher-end concentration greenhouse gas scenario. We analyze the evolution of urban climate, focusing on extreme heat events and the UHI during both day and nighttime periods (UHIN and UHIX respectively). These factors can exacerbate extreme heat events in urban areas (Tan et al., 2010). After this, we assess the vulnerability of both urban and rural areas and populations to climate change. Finally, in Section 4, we provide a summary and conclusion based on our findings.

2. MODELS AND METHODOLOGY

2.1. Modeling configuration

The CPRCM CNRM-AROME is a three-dimensional, non-hydrostatic, bi-spectral, and limited-area model, based on the numerical weather prediction model of Météo-France (Seity et al., 2011). Note that in the following paper, AROME will be used instead of CNRM-AROME. AROME operates for climate modeling applications at a high resolution of 2.5-km of horizontal resolution. It is coupled to the SURFEX land surface modeling system (Masson et al., 2013), which provides a suite of surface parametrization that can be activated based on the land use and land cover. More specifically, SURFEX includes the Town Energy Balance (TEB) urban canopy model in a configuration close to the historical version (Masson, 2000) for urban areas, and the Interaction Soil-Biosphere-Atmosphere (ISBA) model in its version with three soil layers (3-L, Boone et al., 1999) for soils and vegetation. The model's physiographic description is based on the GMTED2010 (Global Multi-resolution Terrain Elevation Data, Carabajal et al., 2011) which has a native horizontal resolution of 250-m, and the land-use mapping is sourced from the ECOCLIMAP-I database (Masson, 2003) at 1-km of horizontal resolution.

As part of the European research project EUCP (Hewitt and Lowe, 2018), AROME has been run over the northwestern part of Europe (see map in Figure 1). The model was first run in an evaluation configuration driven by ERA-Interim over the period 1998-2018, including two years of spin-up. The model setup and the simulation are described in detail in Caillaud et al. (2021), and a general evaluation of the performance of AROME is discussed in Lucas-Picher et al. (2023). The evaluation of AROME reveals systematic biases in the simulation of incident solar radiation, due to an underestimation of cloud cover by the model. As a result, AROME tends to be warmer in both minimum and maximum summer temperatures during summer. Furthermore, the evaluation of AROME shows a cold bias in spring maximum temperatures, which is related to an overestimation of precipitation.

In this study, AROME simulations were conducted over an historical time period ranging from January 1, 1984, to December 31, 2005, and a future period ranging from January 1, 2078, to December 31, 2099 (including two years of spin-up). In this configuration, AROME is forced every hour at its lateral boundaries by the Regional Climate Model (RCM) ALADIN (Nabat et al., 2020), operating at a 12-km horizontal resolution. In turn, ALADIN is driven by the Global Climate Model (GCM) ARPEGE-Climat (Déqué et al., 1994), also known as CNRM-CM5 as part of the CMIP5 initiative, with a horizontal resolution of 1.4° (Voldoire et al., 2013). The RCP8.5 greenhouse gas emission scenario is used for this analysis.

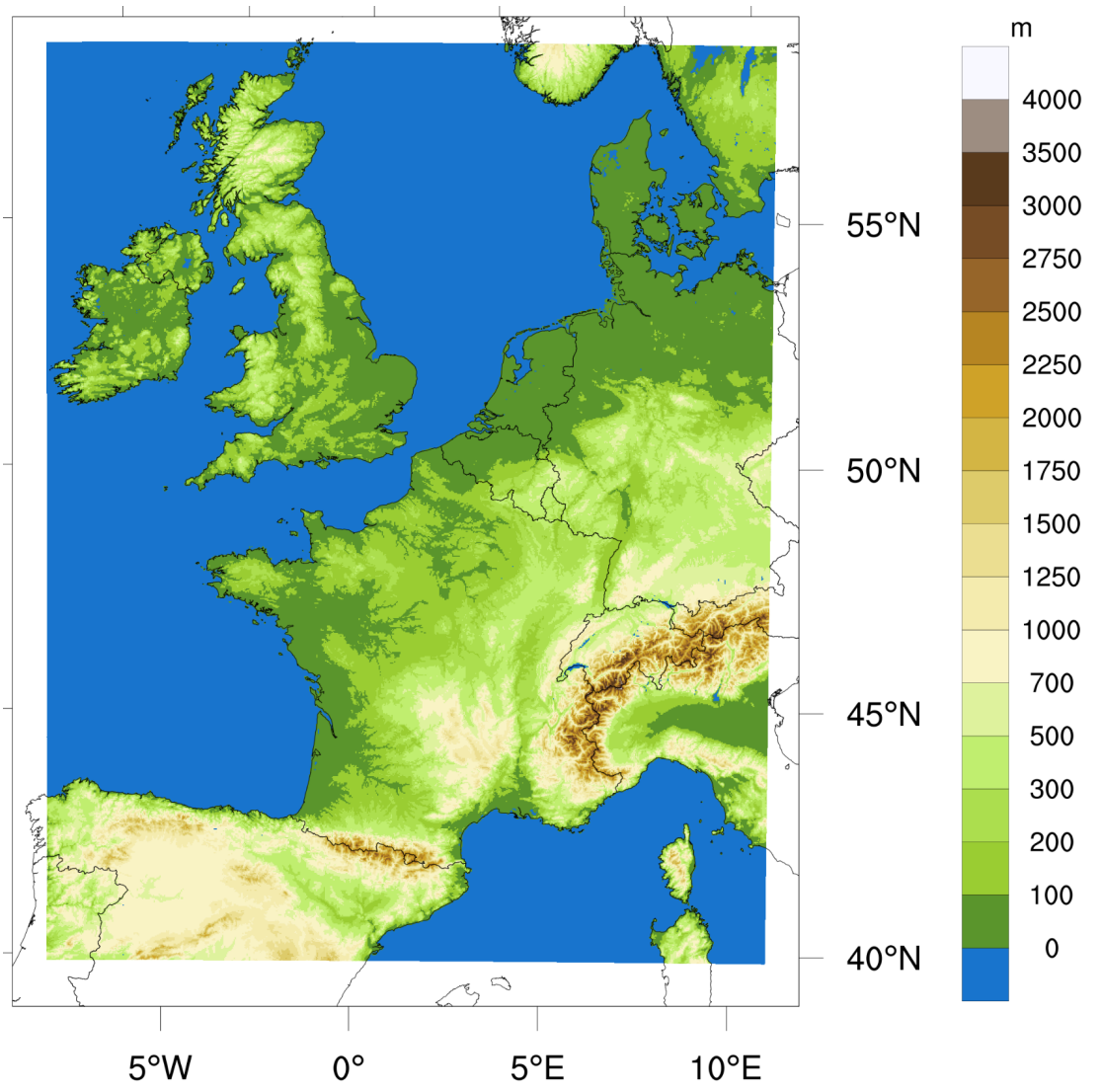

Figure 1. Simulation domain of AROME covering northwestern Europe with a 2.5-km horizontal resolution

2.2. Selection of cities

In this study, we focus on 14 cities within the French metropolitan territory, covered by the simulation domain, that have been studied in Michau et al. (2023). All the cities are among the most populated urban areas in France, and are spread across the region to represent various geographical and climatic conditions.

As the previous study of Michau et al. (2023), these cities were classified according to their climatic zones, following the methodology of Joly et al. (2010). The cities are grouped into four categories based on their climatic characteristics: continental climate cities (CON), including Lyon, Dijon, Nancy, Strasbourg; Mediterranean climate cities (MED), including Marseille, Montpellier, Nice, Nimes; oceanic climate cities (OCE), including Bordeaux, Lille, Nantes, Rennes; and semi-oceanic climate cities (SOCE), including Paris and Toulouse. Figure 2 provides a map of the 14 cities with their climatic zones and the orography shown as background data. Table 1 provides additional information on each of the cities. Note that the climatic zone characteristics are detailed in Michau et al. (2023).

Table 1. Additional information about the 14 selected cities.
| Sources: The population census and the size of metropolitan areas are from INSEE (the French National Institute for Statistics and Economic Research) in 2019. The altimetry information is extracted from the IGN (French National Geographic Institute) digital terrain model at the longitude and latitude coordinates of each city.

Climate zone	City	Altitude (m)	Size of the metropolitan area (km²)	Population (x1000 inhabitants)
OCE	Bordeaux	6	578	814
	Lille	23	672	1 179
	Nantes	21	523	665
	Rennes	24	705	457
CON	Dijon	267	240	255
	Lyon	237	534	1 412
	Nancy	205	142	258
	Strasbourg	136	338	505
MED	Marseille	140	3 149	1 899
	Montpellier	39	422	491
	Nice	13	1 480	550
	Nîmes	76	791	258
SOCE	Paris	31	814	7 094
	Toulouse	144	458	796

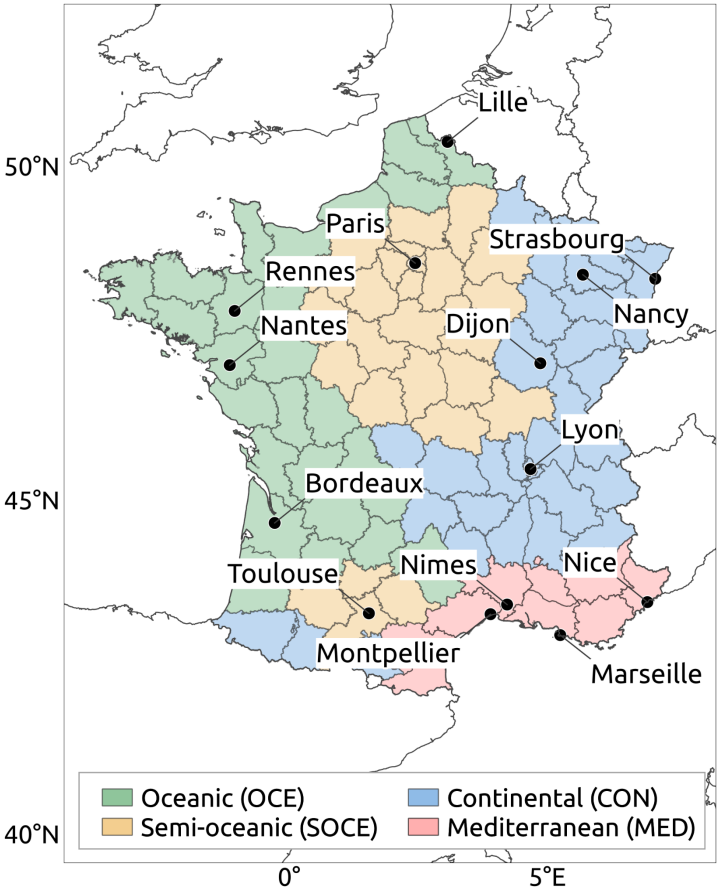

Figure 2. Location of the 14 selected cities in the Metropolitan France area. The climatic zones, based on Joly et al. (2010), are simplified as proposed by Michau et al. (2023).

2.3. Climate indicators for urban vulnerability-oriented studies

2.3.1. Urban heat island intensity

The intensity of the urban heat island is calculated with a daily time step for both nighttime (UHIN) and daytime (UHIX) periods according to:

$$UHIN = TN_{URB} - TN_{RUR} \text{ and } UHIX = TX_{URB} - TX_{RUR} \text{ (in °C)}$$

In each city, TN_{URB} (TX_{URB}) refers to the minimum (maximum) daily temperatures of the most urban grid cell with the objective to calculate the maximum intensity of the UHI. The grid cell selection is done using a systematic check of the land-use fraction based on the ECOCLIMAP-I database (*cf.* Section 2.1) and the distance to the city center. The rural minimum and maximum daily temperatures (TN_{RUR} and TX_{RUR}) are calculated as a spatial average of minimum and maximum temperatures over a rural mask. The reference geographical domain is defined with a diagonal length of 50-km centered on the city (Figure 3, right). The rural mask is the set of grid cells within the domain whose fraction of town and water (based on the ECOCLIMAP-I database) are lower than or equal to 50% and 95% respectively. Additionally, rural grid points differing in altitude from the urban area by more than 750 m are excluded from the spatial average.

The UHIN indicator has been studied by Michau et al. (2023) for the same set of French cities using a retrospective evaluation simulation of AROME over the 2000-2018 period. The simulated UHIN has been compared with long term weather station data to determine the model's ability to reproduce the UHI. This related study concluded that AROME realistically simulates the seasonal variability, minimum and maximum intensities of the nocturnal UHI, and similarities between cities belonging to the same climatic zones.

2.3.2. Heatwaves definition and detection

The heatwave (HW) detection is performed following the methodology developed over metropolitan France and applied to the Euro-CORDEX multi-model ensemble by Ouzeau et al. (2016). This method has the advantage of being applicable to various datasets (observations or models), climatic and geographic context, and sectors. The method is based on threshold exceedances applied over a long time series of mean daily temperature (TM). Three different quantiles are used to define the threshold values over a past reference period of 30 years. A HW event is identified when TM exceeds the 99.5 percentile threshold (Th1). The event lasts before and after the HW peak as long as TM does not fall durably (*i.e.*, more than two consecutive days) below the 97.5 percentile (Th2) and does not fall even occasionally below the 95 percentile (Th3). A HW is described by three main parameters: its duration (in days), its maximum intensity (peak of TM reached during the event, in °C), and its severity (in °C) calculated as the cumulative degrees above Th2 over the duration of the event.

In this study, the past reference period for the quantiles calculation is the 20-year historical period 1986-2005, using the TM time series from the AROME simulation. The quantiles are defined separately for the urban and rural areas of each city. In each city, the urban and rural daily mean temperatures (TM_{URB} and TM_{RUR}) refer to the spatial average of daily temperature time series TM in the urban mask and the rural mask, respectively (Figure 3). The rural mask is defined as before for the calculation of UHIN and UHIX. The urban mask is the set of grid cells within the domain whose fraction of town (based on the ECOCLIMAP-I database) is higher than 50%.

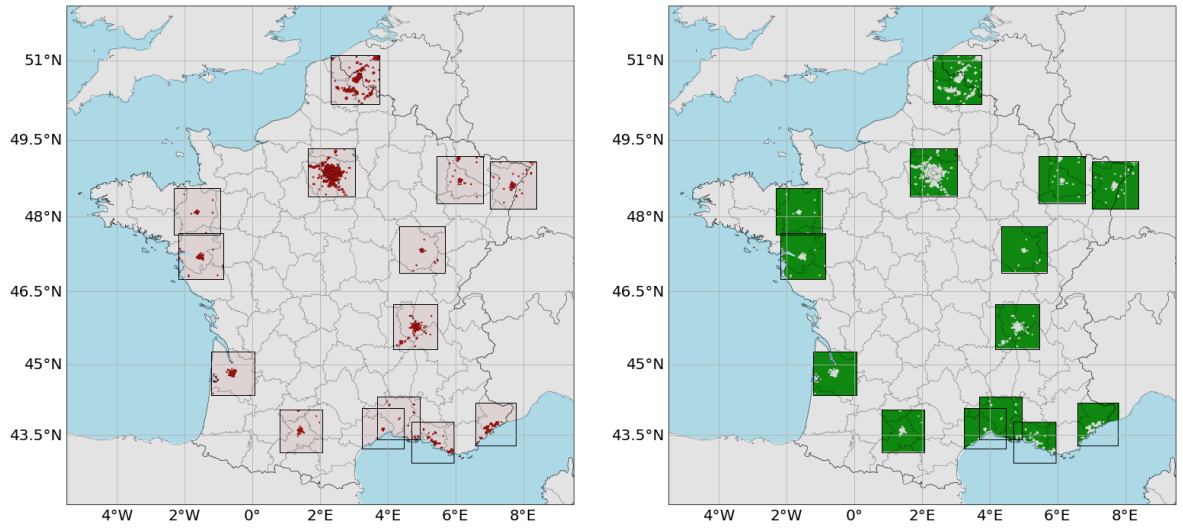

Figure 3. Urban [left] and rural [right] grid points located in the reference geographical area around the city centers.

2.3.3. Evaluation of heatwaves over the historical period

Using the proposed HW indicator, the modeled HWs over the historical period 1986-2005 were compared to the observed HWs with the objective to assess the capacity of AROME to simulate past events. For this purpose, the method was applied to the TM time series from the ANASTASIA gridded observation database in the same way as for the simulation data. The ANASTASIA product (Besson et al., 2019) is a gridded dataset of daily TN and TX daily at 1-km horizontal resolution over Metropolitan France for the time period 1947-2016 (detailed description in Michau et al., 2023). The extracted HWs are compared by limiting the analysis to the rural area to: (1) avoid urban influences which are not precisely represented in the ANASTASIA database since few urban stations were used to develop this observation database, and (2) focus on regional conditions.

We first compared the temperature quantile values (Th1, Th2, Th3) from the observed and simulated TM series used to identify HWs. Table 2 presents the biases between the modeled and the observed thresholds for each city. It shows that AROME systematically underestimates the three thresholds with a range from -1.6 °C to -4.3 °C depending on the city (except for Marseille which has a lower bias). There is no increase in cold bias for the more extreme threshold, the biases being very close for the three thresholds (if compared city by city).

Table 2. HW threshold values calculated on rural environment in AROME CPRCM *simulations forced by CNRM-CM5 using RCP8.5 scenario, compared to ANASTASIA observations over 1986-2005.*

		Th1	**Th2**	**Th3**
		Bias (°C)		
OCE	**Bordeaux**	-2,6	-2,6	-2,8
	Lille	-1,8	-1,6	-1,6
	Nantes	-3,3	-3,4	-3,1
	Rennes	-3,1	-3,0	-2,9
CON	**Dijon**	-3,2	-3,3	-3,1
	Lyon	-3,6	-4,0	-3,8

	Nancy	-2,6	-2,4	-2,3
	Strasbourg	-2,7	-2,6	-2,5
MED	**Marseille**	0,1	-1,4	-1,7
	Montpellier	-2,1	-2,3	-2,5
	Nice	-2,8	-4,0	-4,3
	Nimes	-1,7	-2,1	-2,4
SOCE	**Paris**	-2,7	-2,4	-2,3
	Toulouse	-3,2	-3,5	-3,6

Based on these thresholds that are defined in percentiles, the modeled and observed HWs can be compared without debiasing the model. Figure 4 provides a comparison between the modeled and observed number of HW days as an average per year over the 1986-2005 period for all studied cities, as well as the total number of events. Between 10 and 16 past observed HWs are extracted, with the lowest number occurring in Bordeaux (OCE), and the highest in Nimes (MED) and Toulouse (SOCE). In comparison, AROME simulates between 7 and 14 HWs depending on the climatic and geographical zone. With regard to the number of days, according to the observations, there are fewer days of HWs for cities in oceanic and continental climatic zones (except for the particular case of Lille) than for cities in semi-oceanic and especially Mediterranean climatic zones. These geographic contrasts are less clear in the AROME results. The model tends to slightly overestimate the number of HWs days for most OCE and CON cities and underestimate it for MED cities. Nevertheless, the range of variation obtained with AROME is consistent.

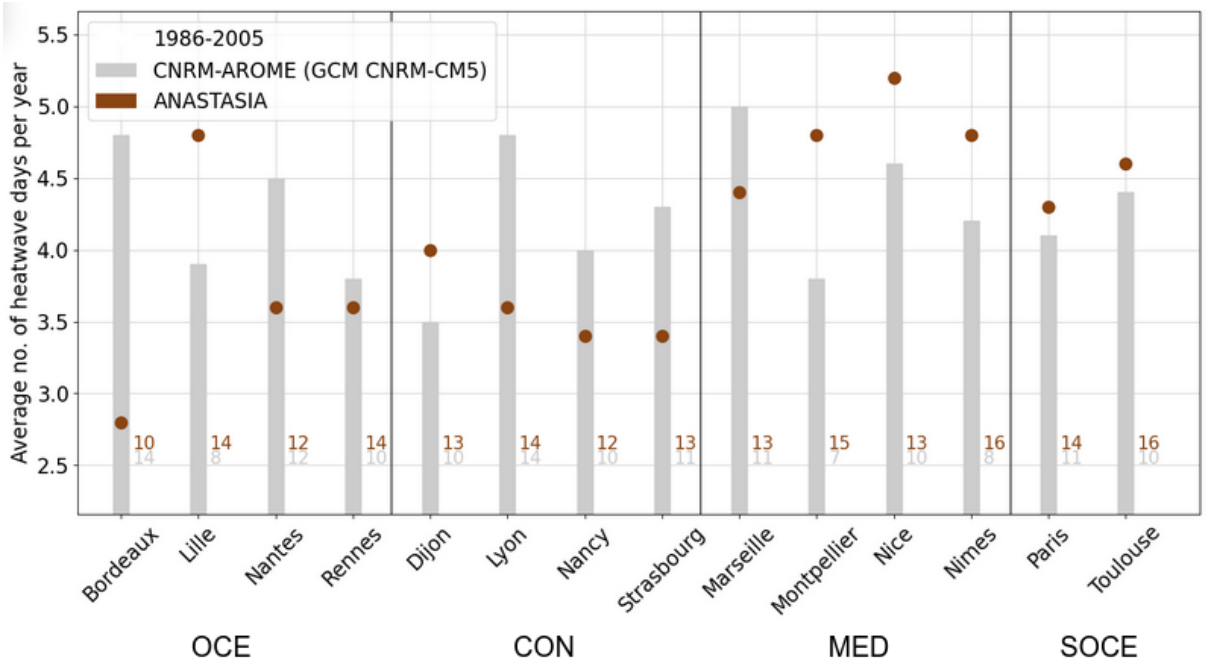

Figure 4. Average no. of HW days per year detected in the rural environment in AROME CPRCM *simulation forced by CNRM-CM5 (light gray), compared to the ANASTASIA observation (dark red) over the period 1986-2005. The total number of observed or simulated HWs are noted at the bottom right of each bar of the bar plot.*

The evaluation of the AROME's capacity to simulate extreme heat events underlines some cold biases in HW thresholds. A complementary analysis of the AROME simulation forced by ERA-Interim observations over 2000-2018 showed rather warm biases for HW thresholds (not shown here), suggesting that the reported biases do not come from the regional climate model. The cold biases are

likely to be attributed to CNRM-CM5 (Voldoire et al., 2013; Lucas-Picher et al., 2023). Despite that, AROME performed well in simulating the number of HWs, as well as their average duration per year during the 1986-2005 period.

Subsequently, the method was applied to the longterm climate simulations using the thresholds defined for the historical period. The objective is to compare the evolution of the exposure of urban and rural environments to heat waves with climate change.

3. RESULTS

3.1. Temperature evolution with climate change

Before analyzing the results at the city-scale, the warming trends over France, and the spatial and seasonal variability of these trends, are studied. The Figure 5 displays seasonal maps of warming in daytime and nighttime temperatures between 1986-2005 and 2080-2099. In addition, seasonal maps of change in the 90th percentile of the diurnal and nighttime temperatures (called hereafter TX90p and TN90p respectively) are presented in Figure 6. The warming over the period 1986-2005 to 2080-2099 shows a significant seasonal variability (Figure 5). The temperature increase varies between +2 and +4 °C in DJF (from December to February) and MAM (from March to May), between +3 and +6 °C in JJA (from June to August), and between +4 and +7 °C in SON (from September to November). According to Michau et al. (2023), several French cities are currently experiencing local climatic and geographical variability. These local spatial disparities are projected to increase with climate change, with a strong shift towards warmer temperatures (Figure 5). The northern half of France is projected to warm less than the southern half of France, especially in TX in JJA. In addition, coastal and mountainous areas such as the Atlantic and Mediterranean coasts, and the Alps, are expected to become warmer than lowland areas (Figure 5).

The analysis of the change of the upper tail of the TN and TX spatial distribution (Figure 6) confirms this trend in a more pronounced way. TN90p and TX90p are projected to increase strongly in coastal and mountainous areas, especially in the diurnal temperature (*e.g.*, +9 on the southern half of the Atlantic coast). In the Mediterranean region, the projected increase in extreme warm temperatures is substantial, ranging from +5 to +9 °C in JJA (Figure 6). Our findings are consistent with Christidis et al. (2015), which shows using several CMIP5 models, covering a region including France, Germany and Italy, that RCP8.5 projects a warming from +8 to +10 °C for the upper tail of summer mean temperature by the end of the century. These results are also consistent with the work of Giorgi (2006) and Diffenbaugh and Giorgi (2012), which identified the Mediterranean region as a “hot spot” for climate change.

These results highlight that the warming resulting from climate change (according to RCP8.5 emission scenario) is marked by significant spatial and seasonal variability over the French territory, which suggests that cities depending on their location will be impacted in different ways. As part of the study, several perspectives concerning HWs will be investigated, both through a practical application to the city of Paris (SOCE), and through a generalization to the 13 other selected French cities. In Section 3.2.1, the aim is to analyze the characteristics of HW according to whether they are extracted for urban areas or surrounding rural areas. In Section 3.3.1, the aim is to analyze the differentiated exposure of urban and rural areas to HW with climate change.

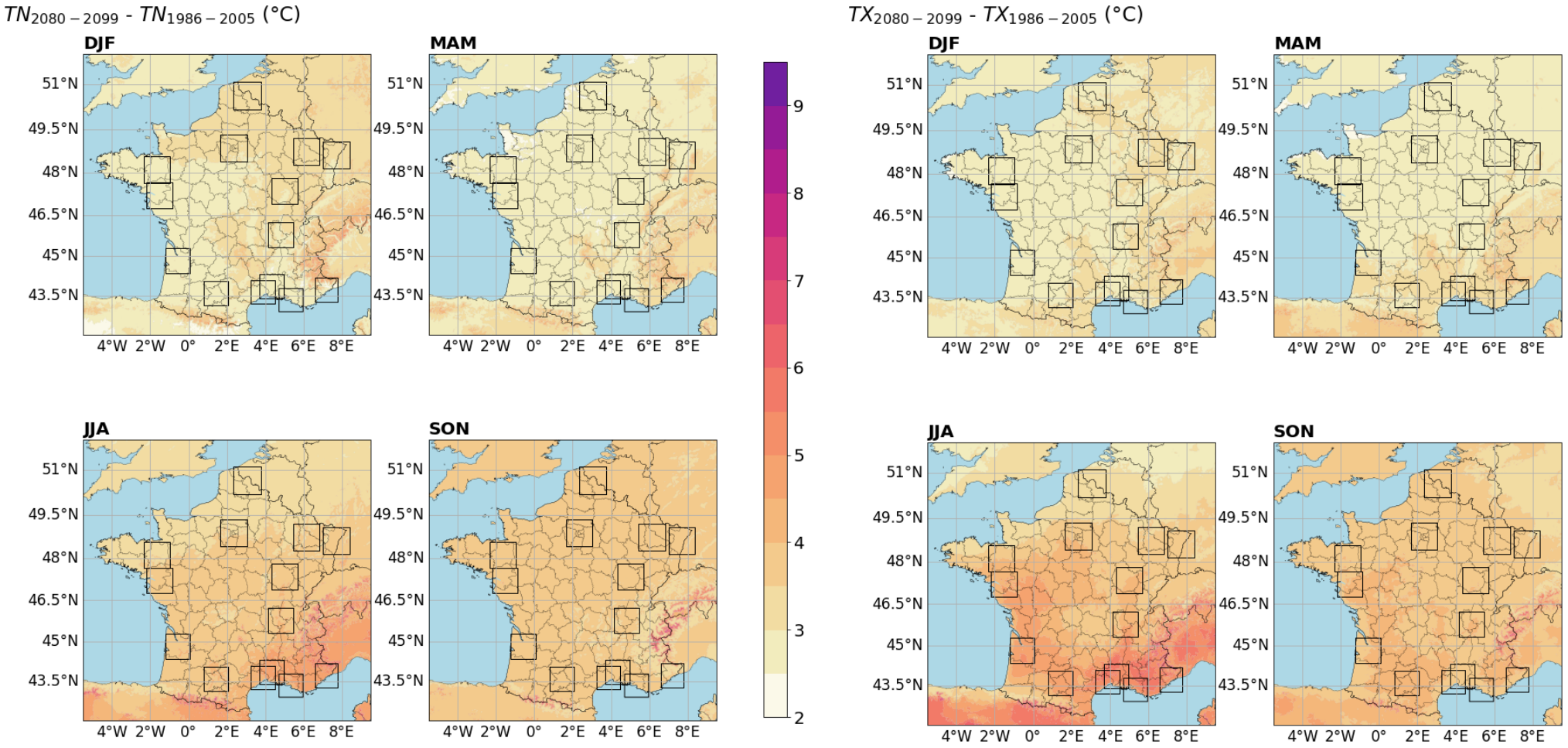

Figure 5. Multi-year seasonal minimum [left] and maximum [right] temperatures differences (in °C) between 1986-2005 and 2080-2099 over metropolitan France. The reference geographical domains for each city are shown with black squares.

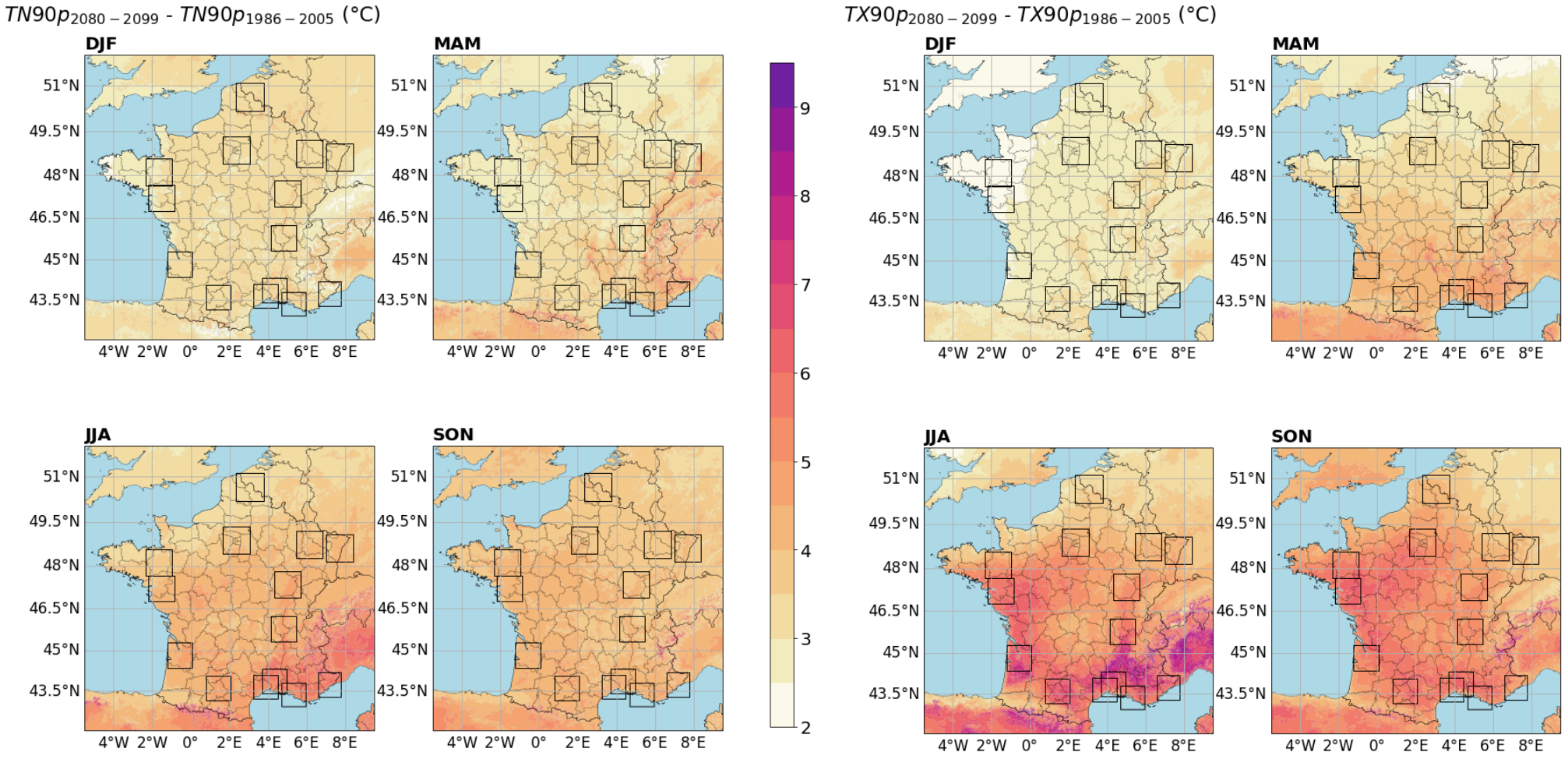

Figure 6. Multi-year seasonal 90th percentile minimum [left] and maximum [right] temperatures differences (in °C) between 1986-2006 and 2080-2099 over metropolitan France. The reference geographical domain is shown in black.

3.2. Urban-rural contrast in heatwaves exposure

3.2.1. Case study of the city of Paris (SOCE)

Figure 6. Simulated HWs (bubble) in Paris over 1986-2005 [left] and 2080-2099 [right] periods, in urban (red) and rural (green) areas. HWs are characterized by their maximum intensity (y-axis), duration (x-axis) and severity (bubble size). Remember that HW are detected using mean temperatures. The total number of HW for both environments and periods is specified at the top left, while the thresholds calculated over the 1986-2005 period are indicated at the bottom left.

With Paris as a case study, the HWs identified over the historical period for both urban and rural areas (with specific thresholds for each) are compared on the basis of a bubble chart (Figure 6, left). Over this period, 12 HWs (4 HW days per year according to further analysis) are simulated in urban areas compared to 11 HWs (4.1 HW days per year according to Figure 4) in rural areas. The contrast between urban and rural environments can be attributed to the lower day-night temperature variability in the city induced by the urban overheating, which prevents the temperature from falling down below the thresholds for a prolonged period. Both sets of HWs are very comparable in terms of number of occurrences and number of days. However, the maximum intensity of HWs is systematically higher in urban areas than in rural areas because the detection thresholds are higher (+0.8, +1.3 and +1.2 °C for Th1, Th2 and Th3, respectively). This results from the UHI effect that shifts the TM distribution over the historical period, which is used to calculate the percentile thresholds over urban areas, towards warmer temperatures.

In addition, the magnitude of both nighttime and daytime UHI was calculated and averaged for HW days, as illustrated in Figure 7. The UHI is maximum over the Paris city core where it reaches around +3 °C at night and during the day. If the UHI during HW is averaged spatially over the entire urban area (hatched area in Figure 7), its intensities are close to the shifts observed on the HW detection thresholds between urban and rural areas.

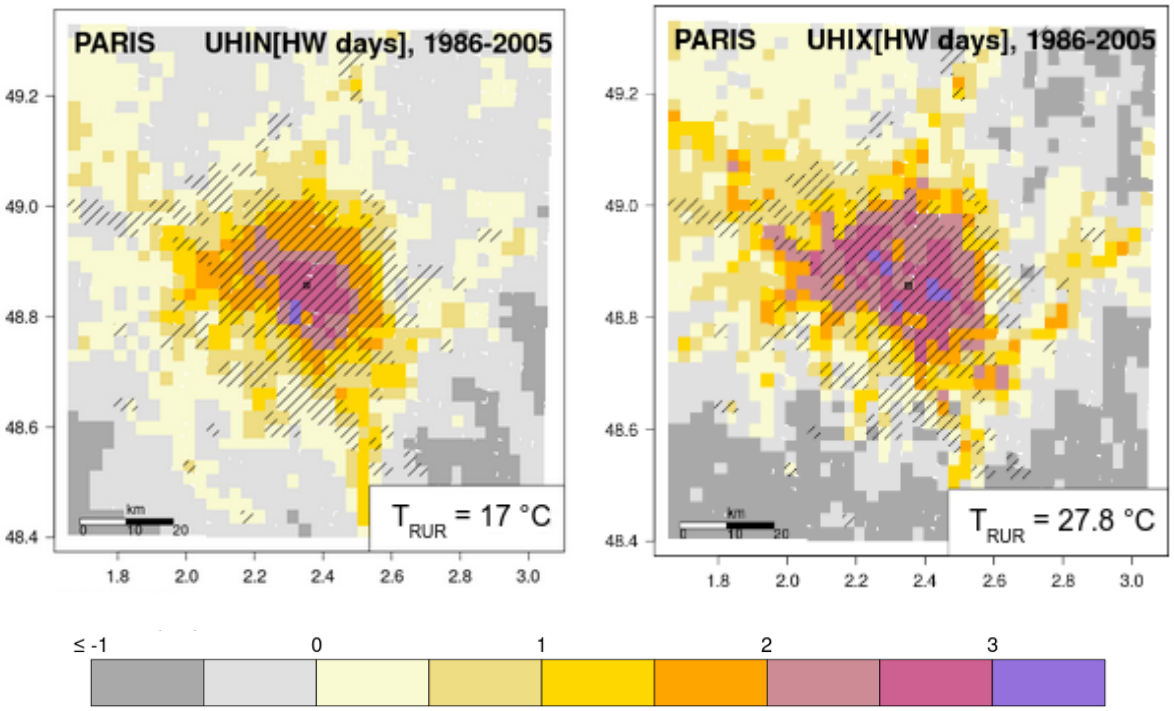

Figure 7. Nighttime [left] and daytime [right] UHI (in °C) during HW days over 1986-2005 period maps in Paris. Urban areas are indicated by hatching.

3.2.2. Results for the other cities

For each city of interest, the HW detection is performed and HWs are extracted for the urban area and the associated rural area. In this section, the characteristics of modelled HWs over the 1986-2005 period are analyzed. Figure 8 displays the distribution of HW duration and maximum intensity in the 1986-2005 and 2080-2099 periods.

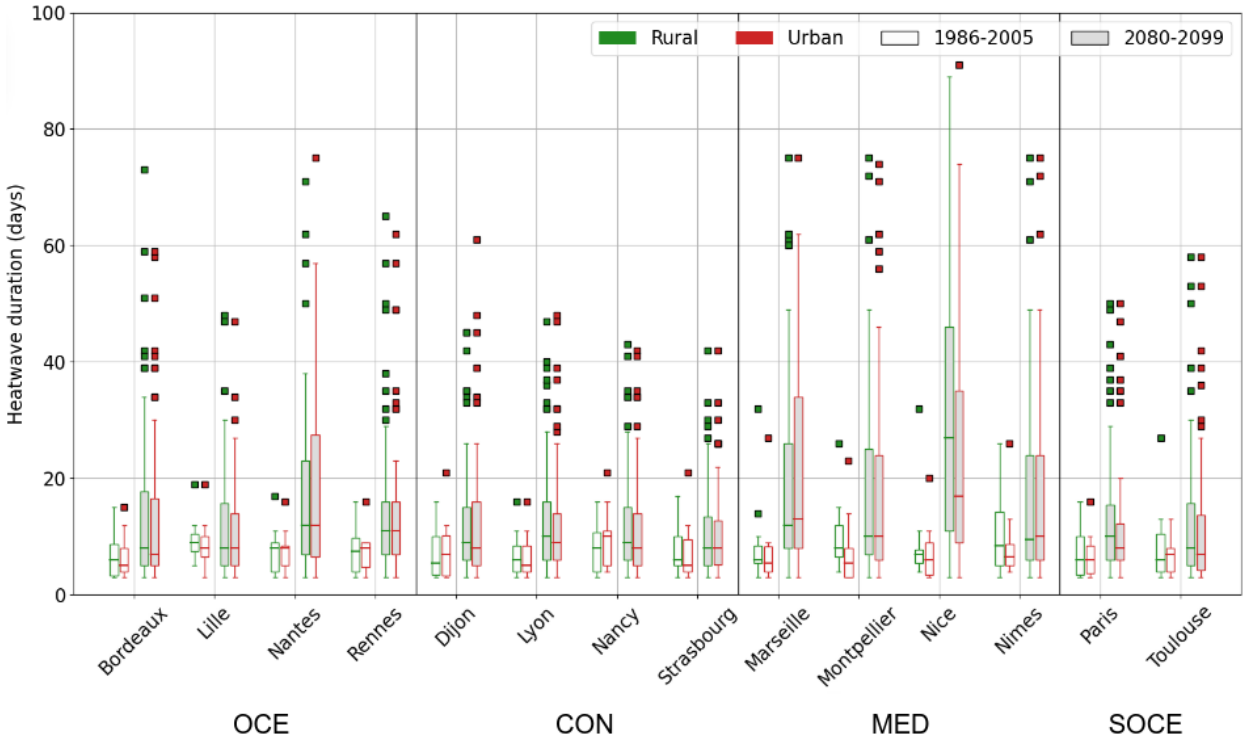

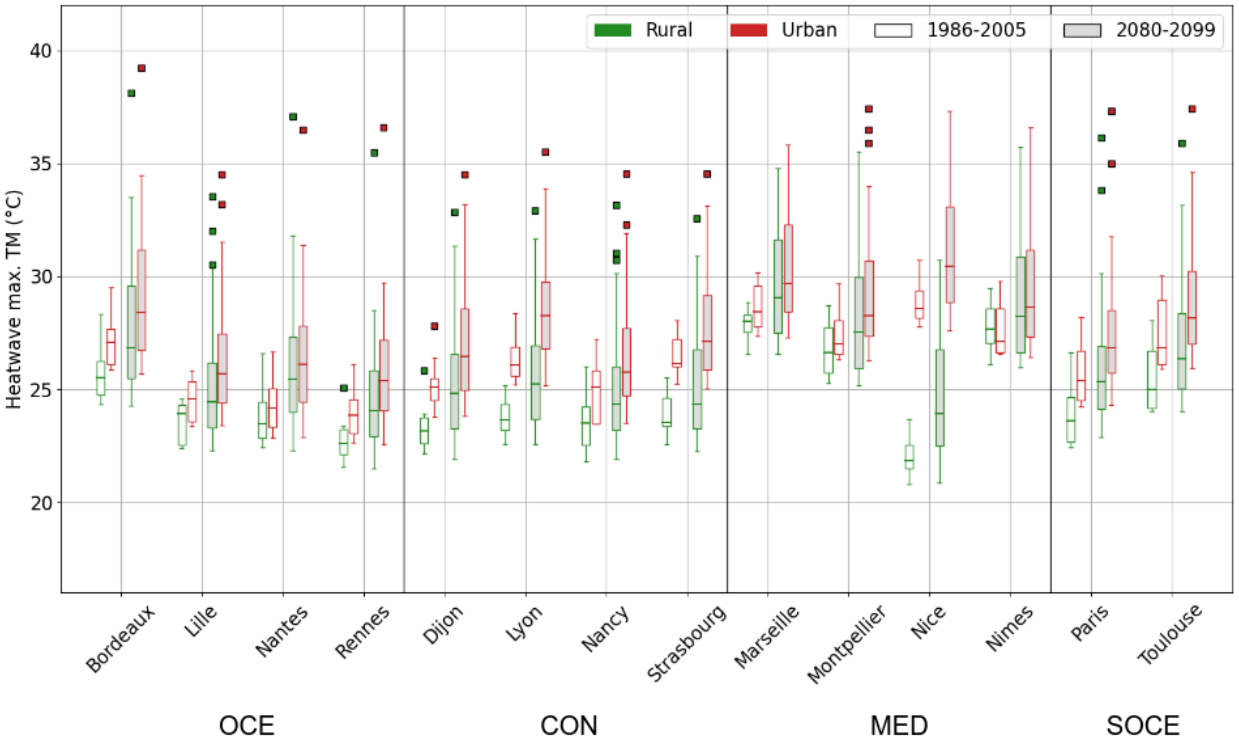

Figure 8. HW duration (in days) [top] and maximum intensity [bottom] in urban (red) and rural (green) areas over 1986-2005 (white background), and 2080-2099 (gray background) periods for each city. Remember that HW are detected using mean temperatures.

The duration of extreme heat events (Figure 8, top) varies between urban and rural areas over the period 1986-2005. The median duration is generally slightly higher in rural areas, with the exception of Rennes (OCE), Dijon (CON), and Nancy (CON). However, the distribution of the HW duration is relatively homogeneous in both areas, with events slightly scattered around the median, as observed in Nice (MED). It should be noted that the sample size consists only of the 20-year span of the period 1986-2005, which counts few extreme heat events (as shown using ANASTASIA observation database in Figure 4). The sample size is quite small for further discussion. Nevertheless, these results provide a useful basis for assessing changes in extreme heat events with climate change.

As for Paris, the median maximum intensities of HWs in the 1986-2005 period are systematically higher in urban areas than in rural areas for all cities. Again, this is caused by the daytime and nighttime UHI (as presented in Table 3). The UHIs calculated for HW days for all cities are systematically positive over the period 1986-2005, with Lyon (CON) having the highest daytime and nighttime UHI of 3.88 and 4.41 °C respectively. Figure 8 also shows a significant climatic and geographical variability, with higher maximum intensities in the southern part of France, such as in Bordeaux (OCE), Lyon (CON) or Marseille (MED), than in the northern part of France. This is consistent with the previous study by Soubeyroux et al. (2016), which found strong regional differences in HW maximum intensity over metropolitan France. The southern half of France, including the Mediterranean region, reflects typical climatic conditions characterized by a distribution of HW maximum intensity above 25 °C.

Table 3. Nocturnal and diurnal HW days UHI changes (in °C) for HIST and LONG periods. Biases are indicated by colors ranging from dark blue for negative biases to dark red for positive biases. Non-significant biases around 0 are indicated in white.

		UHIN (°C)			UHIX (°C)		
		1986-2005	2080-2099	2080-2099 - 1986-2005	1986-2005	2080-2099	2080-2099 - 1986-2005
OCE	Bordeaux	1,99	1,77	**-0,21**	2,05	1,72	**-0,33**
	Lille	1,96	1,99	**0,03**	1,75	1,82	**0,07**
	Nantes	1,28	1,20	**-0,08**	2,00	1,60	**-0,40**
	Rennes	1,36	1,18	**-0,18**	2,07	1,86	**-0,20**
CON	Dijon	2,43	2,15	**-0,29**	2,78	2,26	**-0,51**
	Lyon	3,88	3,73	**-0,15**	4,41	3,90	**-0,52**
	Nancy	1,54	1,56	**0,02**	2,08	2,00	**-0,08**
	Strasbourg	2,64	2,53	**-0,11**	3,77	3,64	**-0,13**
MED	Marseille	2,73	2,44	**-0,29**	0,94	0,56	**-0,38**
	Montpellier	2,07	2,01	**-0,06**	1,53	1,77	**0,24**
	Nice	8,94	8,35	**-0,59**	6,17	5,48	**-0,69**
	Nimes	1,42	1,32	**-0,10**	1,83	1,79	**-0,04**
SOCE	Paris	2,94	2,61	**-0,33**	2,40	1,93	**-0,47**
	Toulouse	2,12	1,97	**-0,15**	2,34	1,91	**-0,43**

3.3. Evolution of heatwaves exposure with climate change

3.3.1. Case study of the city of Paris (SOCE)

The comparison of HWs detected for the Paris region for the historical period 1985-2006 and the long-term period 2080-2099 with RCP8.5 shows an increase of the frequency of HWs in both urban and rural areas by about 6 times with climate change (Figure 6, right). Figure 6 also shows a significant increase in the duration of HWs, with several events lasting more than a month. This finding is in agreement with Brown (2020), who projected a 130% increase in the duration of HW in Paris based on a rate of about 10 days in the historical period, using an ensemble of GCM from CMIP5 forced with the RCP8.5 scenario. Finally, for a majority of HWs, the maximum intensity of the event increases at the end of the century.

For Paris, 68 events are reported in urban areas and 63 in rural areas for the last two decades of the 21st century, *i.e.* an average of 3.40 and 3.15 events per year. But while there are more HWs detected in urban areas, the events are rather longer in rural areas (see Paris' boxplot in Figure 8, top), so that the cumulative number of HW days is slightly higher (as shown in Figure 10). The bubble chart also shows that the differences in maximum intensity between urban and rural HWs appear to be narrowing for a number of late-century events. In conclusion, we can see that for Paris both the intensity and duration of HWs are increasing more in rural areas than in urban areas with climate change under the RCP8.5 scenario.

Temperatures remain higher overall in urban areas than in rural areas, with average UHIs at night and during the day of 2.61 °C and 1.93 °C, respectively (Table 3). Nevertheless, the intensity of UHIs decreases by -0.33 °C at night and -0.47 °C during the day between 1986-2005 and 2080-2099. The spatial evolution with climate change of the daytime and nighttime UHI during HW days is mapped in Figure 9. The UHIs decrease in response to an increase of background temperature T_{RUR} with spatial variation, by +0.6 and +1.2 °C during the day and night respectively.

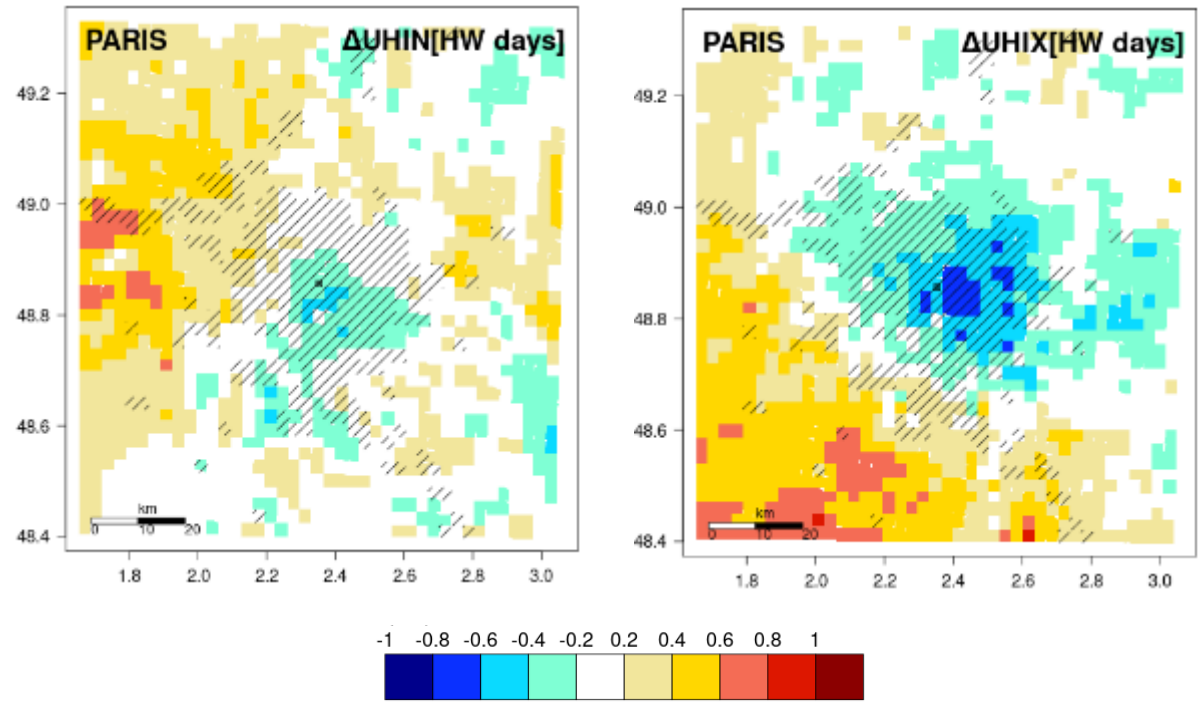

Figure 9. Nighttime [left] and daytime [right] UHI differences (in °C) during HW days between 1996-2005 and 2080-2099 periods maps in Paris. Urban areas are indicated by hatching.

3.3.2. Evolution of HW for the other cities

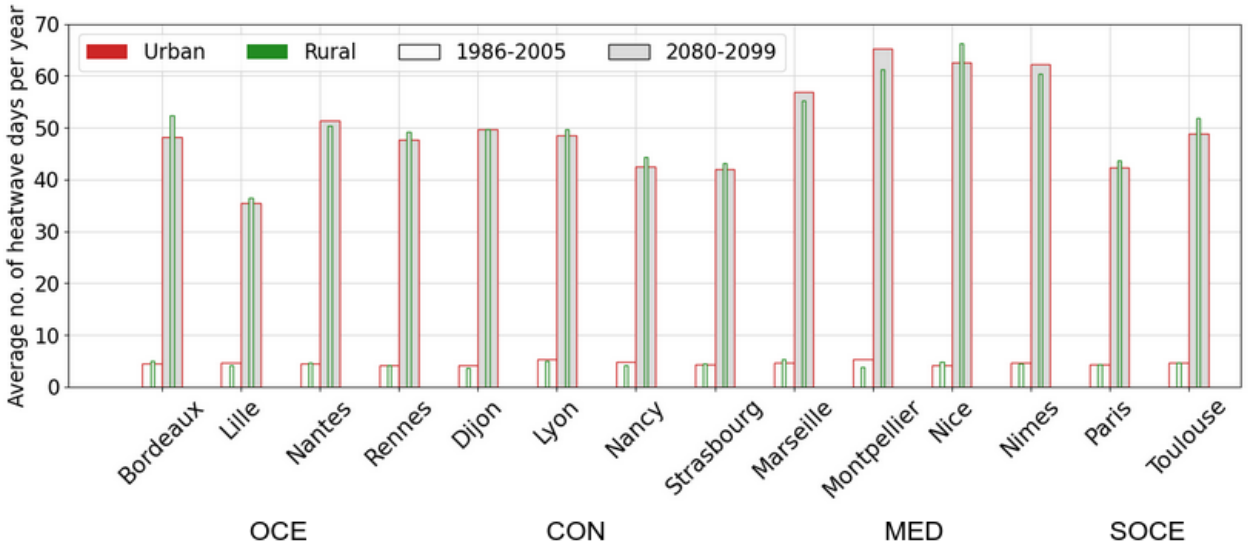

Figure 10. Average no. of heatwave days per year in urban (red) and rural (green) areas over 1986-2005 (white background), and 2080-2099 (gray background) periods for each city.

The analysis of the HW evolution is extended to all cities. The average number of HW days per year over the 1986-2005 period ranges between 3.5 and 5 days in both urban and rural areas (Figure 4), with no clear pattern emerging in relation to climate and geographical areas. With climate change, the number of HW days increases by a factor of 7 to 14 (Figure 10). These differences in the increase in the number of HW days are consistent with the variability of warming trends over the French metropolitan area (as discussed in Section 3.1). The smallest increase is observed for the northernmost cities, especially for Lille (OCE), but also Nancy, Strasbourg (both CON) and Paris (SOCE) that experience the smallest warming trends according to Section 3.1. On the contrary, the largest increase in HW days is observed for

the Mediterranean cities (Montpellier, Nice, Nimes, and to a lesser extent, Marseille), that experience a strong warming between 1986-2005 and 2080-2099 (Section 3.1). Nantes, Rennes, and Bordeaux (all three in OCE), located close to the Atlantic coast, as well as Toulouse (SOCE), located in the south of France, also experience a significant increase in HW days until the end of the century, in response to a strong warming, especially in JJA (Section 3.1).

The results also provide clear evidence of a significant shift in the distribution of HW duration across in both urban and rural areas due to climate change for all cities (Figure 8, top). The most notable changes occur in the Mediterranean region, in accordance with Fischer and Schär (2010), where HWs lasting three weeks or more are becoming much more frequent. The median of HW duration increases slightly in both urban and rural areas, with the exception of the urban area of Nancy (CON) and the rural area of Nantes (OCE). The distribution of HW maximum intensity increases in both urban and rural areas of most cities (at the top of Figure 8). The median increases by between +0.6 and +2.2 °C in urban areas and by between +0.5 and +2.1 °C in rural areas. Again, the largest increases are seen in the Mediterranean cities. The behavior of Nice (MED) may not be well captured in both periods, possibly due to the complex topographic context previously highlighted in Michau et al. (2023).

The comparison between urban and rural areas highlights that the projected changes in HW days (Figure 10) are slightly greater in rural areas than in urban areas, for most cities (except for the Mediterranean cities of Montpellier, Nîmes, and Marseille). Additional analyses suggest that this is a response to a significant increase in rural temperatures in JJA (not shown here). Based on studies of historical extreme heat events, high temperatures in rural areas are mainly due to significant soil dryness (Beniston, 2004), which reduces evaporation from vegetation that cools the air (Zampieri et al., 2009). Several factors, depending mainly on large-scale dynamical processes (*e.g.*, anomalous SST studied in Feudale and Shukla, 2010), could explain the dry conditions, such as record temperatures, below-normal precipitation (Ferranti and Viterbo, 2006), specific wind circulations, and more. Also, even if the maximum intensity of HWs remains generally more pronounced in urban areas than in rural areas in all cities (Figure 8, bottom), the gap between the two environments (urban and rural) is narrowing compared to the differences in maximum intensities noted over the historical period due to the general decrease of UHI for all cities (as shown in Table 3). By the end of the century, the UHIs calculated for HW days are projected to decrease by less than -1 °C, with climatic and geographical variation. The reduction of UHI intensities in JJA has already been projected in previous climate change studies. For example, in Europe, Lemonsu et al. (2013), Hamdi et al. (2013, 2016), and McCarthy et al. (2012) found a reduction in nighttime and daytime UHI intensities in Paris, Brussels, and London, respectively. Further analysis shows that urban temperatures warm slightly less than rural temperatures under climate, in line with Fischer et al. (2012) and Oleson et al. (2010). This could be caused by a lack of precipitation and/or a soil moisture depletion leading to a decrease in evapotranspiration as shown by several studies (Oleson, 2012; Mueller and Seneviratne, 2012; Miralles et al., 2014; Hamdi et al., 2015; Kong et al., 2021).

Finally, the evolution of the calendar range of occurrence of HWs between 1986-2005 and 2080-2099 is also analyzed for the different cities (Figure 11). In most cities, HWs start in June and end in September over the period 1986-2005. They are more common in August, with a maximum frequency of 20%. In most of the cities, HWs are simulated on an extended HW period at the end of the century in both urban and rural areas, ranging from early May to late September. There are climatic and geographical disparities, mainly in the length of time HWs last and in the frequency with which these phenomena occur. The calendar range of the occurrence of HWs is more extensive in Bordeaux, Nantes, Rennes and to a lesser extent in Lille (all four in OCE), where the first early HWs are simulated at the end of April. In other cities they appear later, especially in SOCE, where the first HW start in June. Mediterranean cities stand out with maximum HWs frequency around 90% in mid-July, while other cities are around 70% in

the same month. The results are particularly impressive in the cities belonging to the Mediterranean region, as the frequency of HWs is higher than 80% between the middle of July and the middle of August.

The difference between urban and rural areas in the calendar range of HW occurrence over the period 1986-2005 is relatively small (less than 2%). However, where it exists, the HWs frequency is highest in the rural area. By the end of the century, the urban and rural contrast is strengthening, especially between August and October. In Bordeaux and Lille (both OCE), Dijon and Nancy (both CON), and in Paris and Toulouse (both SOCE), Figure 11 shows that rural areas are more subject to late HWs than urban areas (by between +5 to +10%). The Mediterranean cities (except Nice) show a less marked urban/rural contrast.

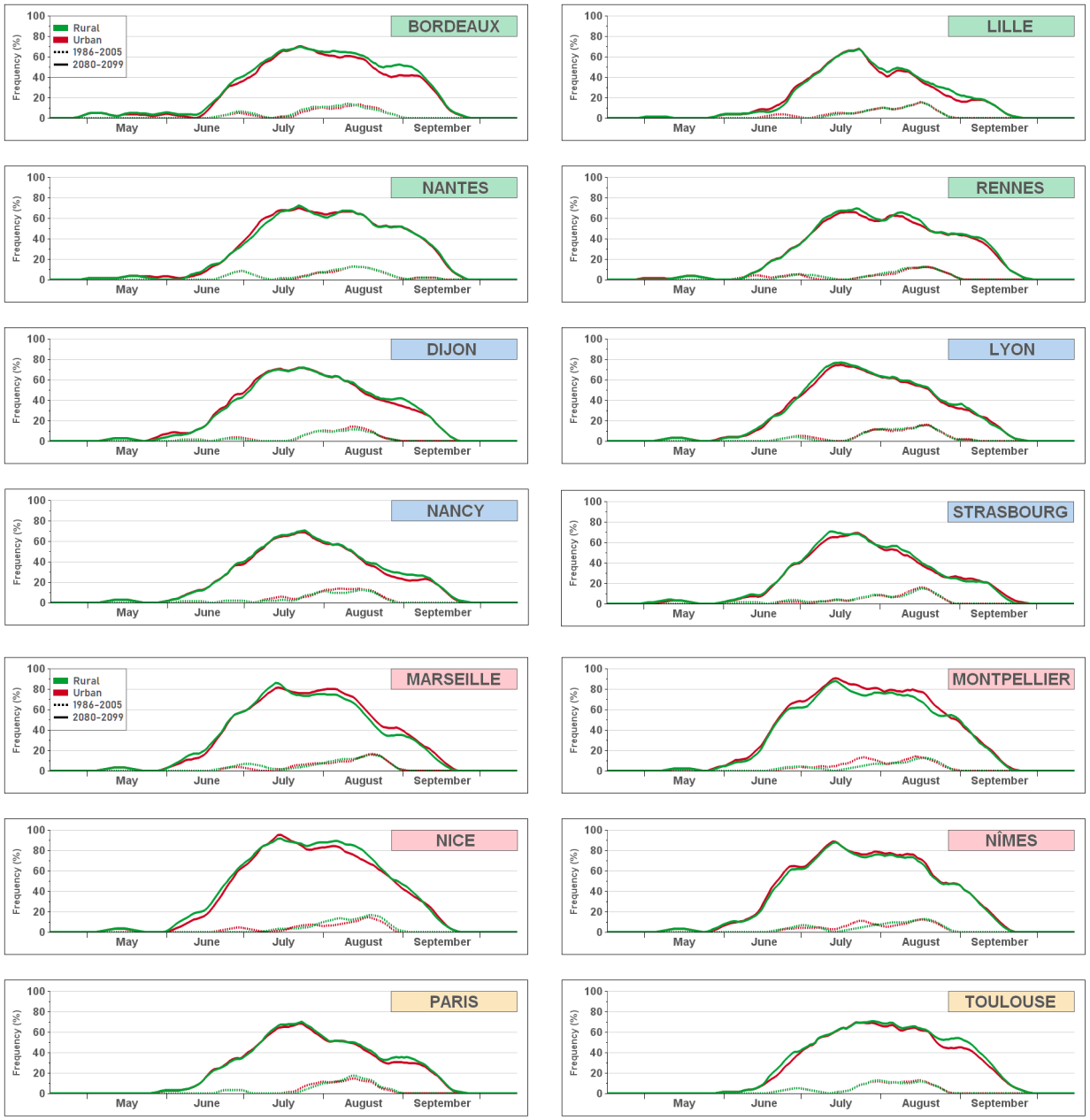

Figure 11. Heatwave days frequency (in %) between April to October in urban (in red) and rural (in green) areas over the periods 1986-2005 (in dotted line) and 2080-2099 (in solid line) for each city.

SUMMARY AND CONCLUSION

This study takes advantage of 20-years of the online coupling of the urban canopy model TEB with the high-resolution climate model AROME over ongoing 20-years periods to study the exposure of French cities to the evolution of HWs with climate change (under the RCP8.5 scenario). Our findings suggest that urban and rural areas will respond differently to climate change. More specifically, both UHIN and UHIX during heatwave conditions are decreasing by the end of the century with climatic and geographical variability responding to temperature changes in urban and rural areas. Rural areas are projected to experience greater temperature increases than urban areas probably due to changes in rural physical processes, such as soil moisture depletion, which could affect the cooling capabilities of the rural environment.

Despite the decrease in UHI until the end of the century, our study projects that HW will become more frequent, longer, and more intense in urban areas due to the pronounced increase in urban temperatures following global warming. Previous studies have also reported that urban areas will experience significantly more warm nights than rural areas by the end of the century (Oleson, 2012; McCarthy et al., 2010). Our findings show that hot weather events will become more frequent, more intense, and more persistent in the Mediterranean region in the context of climate change, in line with Perkins-Kirkpatrick and Gibson (2017). This region is already experiencing the impacts of extreme weather events, such as HW (Baccini et al., 2009), and the populations are highly vulnerable. As the climate continues to warm, this vulnerability will continue to increase. These findings have significant implications for urban planning, highlighting the urgent need to develop effective strategies to adapt to a changing climate and reduce the negative impacts of extreme hot events on human health and well-being.

While our study provides important insights into the potential impacts of climate change on heatwaves, it is important to acknowledge the uncertainty inherent in such projections. The complexity of the climate system, as well as the limitations in the numerical tools used and the difficulty of simulating local-scale processes contribute to this uncertainty.

It is worth noting that our study focused on the RCP8.5 scenario, which is considered the higher end greenhouse gas concentration scenario due to high CO_2 emissions, and not necessarily the most probable one. The plausibility of such a high CO_2 scenario is debated in the literature, but it is still valuable because of the uncertainty in carbon-cycle feedback. Therefore, it seems necessary to specify that the results are probably among the worst that could happen. Next, it would be interesting to apply our methodology to multiple greenhouse gas scenarios to assess the range of possible outcomes. Another approach would be to assess the impacts of climate change on the basis of specific global temperature changes (*e.g.*, +2, +4, or +6 °C).

Furthermore, it is important to note that our study uses a complex modelling chain including a global climate model, a regional climate model, and a very high-resolution climate model. While this configuration allows the investigation of meteorological and climatic conditions related to the urban climate, as well as the complex interaction between local and regional environments, it also introduces the possibility of bias transfer and inconsistencies (Boé et al., 2020). Although uncertainties were reduced through several improvements of individual models, there is still potential for errors associated with the model and the internal variability of the climate. Therefore, the methodology should be generalized to an ensemble of European CPRCMs within the framework of the CORDEX flagship pilot study URB-RCC (URBan environments and Regional Climate Change) in order to support the results obtained here and to reduce the errors associated with the model and the internal climate variability.

ACKNOWLEDGEMENTS

This research has received support from the French National Agency under the future investment program ANR-18-MPGA-0005 and from the EUCP (European Climate Prediction System) project. The EUCP project has been funded by the European Union's Horizon 2020 research and innovation program under grant agreement No. 776613.

The development of the AROME model is the result of a collaboration between CNRM and CNRS laboratories involved in Meso-NH research, along with the international ACCORD consortium. The author thanks Antoinette Alias for her valuable contributions to the development of CNRM-AROME and for conducting multiple simulations using the model. The author also thanks Météo-France for providing the ANASTASIA database.

AUTHOR'S CONTRIBUTIONS

Yohanna Michau: Data collection, Data analysis, Methodology, Visualization, Writing (an original draft), Writing-review and editing.

Aude Lemonsu: Methodology, Writing-review and editing.

Philippe Lucas-Picher: Methodology, Writing-review and editing.

Michel Schneider: Methodology, Visualization, Writing-review and editing.

Cécile Caillaud: Performing CNRM-AROME simulations, Writing-review and editing.

Availability of data and materials

The datasets generated during and/or analyzed during the current study are available from the corresponding author on reasonable request.

REFERENCES

Argüeso D, Evans JP, Fita L, Bormann KJ, **2013**. Temperature response to future urbanization and climate change. *Climate Dynamics, Springer Science and Business Media LLC, 42*, 2183-2199. doi: 10.1007/s00382-013-1789-6.

Baccini M, Kosatsky T, Analitis A, Anderson HR, D'Ovidio M, Menne B, Michelozzi P, Biggeri A, **2009**. Impact of heat on mortality in 15 European cities: attributable deaths under different weather scenarios. *Journal of Epidemiology Community Health, BMJ, 65*, 64-70. doi: 10.1136/jech.2008.085639.

Baniassadi A, Heusinger J, Sailor DJ, **2018**. Energy efficiency vs resiliency to extreme heat and power outages: The role of evolving building energy codes. *Building and Environment, Elsevier BV, 139*, 86-94. doi: 10.1016/j.buildenv.2018.05.024.

Beniston M, **2004**. The 2003 heat wave in Europe: A shape of things to come? An analysis based on Swiss climatological data and model simulations. *Geophysical Research Letters, American Geophysical Union (AGU), 31.* doi: 10.1029/2003gl018857.

Besson F, Dubuisson B, Etchevers P, Gibelin A-L, Lassegues P, Schneider M, Vincendon B, **2019**. Climate monitoring and heat and cold waves detection over France using a new spatialization of daily temperature extremes from 1947 to present. *Advances in Science and Research, Copernicus GmbH, 16*, 149-156. doi: 10.5194/asr-16-149-2019.

Boé J, Somot S, Corre L, Nabat P, **2020**. Large discrepancies in summer climate change over Europe as projected by global and regional climate models: causes and consequences. *Clim Dyn 54,* 2981–3002. doi: 10.1007/s00382-020-05153-1.

Boone A, Calvet J-C, Noilhan J, **1999**. Inclusion of a Third Soil Layer in a Land Surface Scheme Using the Force–Restore Method. *Journal of Applied Meteorology, American Meteorological Society, 38*, 1611-1630. doi: 10.1175/1520-0450(1999)038<1611:ioatsl>2.0.co;2.

Brown SJ, **2020**. Future changes in heatwave severity, duration and frequency due to climate change for the most populous cities. *Weather and Climate Extremes, Elsevier BV, 30*. doi: 10.1016/j.wace.2020.100278.

Caillaud C, Somot S, Alias A, Bernard-Bouissières I, Fumière Q, Laurantin O, Seity Y, Ducrocq V, **2021**. Modelling Mediterranean heavy precipitation events at climate scale: an object-oriented evaluation of the CNRM-AROME convection-permitting regional climate model. *Clim Dyn* 56, 1717–1752. doi: 10.1007/s00382-020-05558-y.

Carabajal CC, Harding D.J, Boy J-P, Danielson JJ Gesch DB, Suchdeo VP, **2011**. Evaluation of the Global Multi-Resolution Terrain Elevation Data 2010 (GMTED2010) using ICESat geodetic control. *International Symposium on Lidar and Radar Mapping 2011: Technologies and Applications, SPIE.* doi: 10.1117/12.912776.

Christidis N, Jones GS, Stott PA, **2015**. Dramatically increasing chance of extremely hot summers since the 2003 European heatwave. *Nature Climate Change, Springer Science and Business Media LLC, 5*, 46-50. doi: 10.1038/nclimate2468.

Copernicus Climate Change Service. OBSERVER: A wrap-up of Europe's summer 2022 heatwave, https://www.copernicus.eu/en/news/news/observer-wrap-europes-summer-2022-heatwave. (22/09/2022)

Daniel M, Lemonsu A, Viguié V, **2018**. Role of watering practices in large-scale urban planning strategies to face the heat-wave risk in future climate. *Urban Climate, Elsevier BV, 23*, 287-308. doi: 10.1016/j.uclim.2016.11.001.

Déqué M & Somot S, **2008**. Analysis of heavy precipitation for France using high resolution ALADIN RCM simulations. *Idöjaras Quaterly Journal of the Hungarian Meteorological Service, 112*, 179-190.

Diffenbaugh NS & Giorgi F, **2012**. Climate change hotspots in the CMIP5 global climate model ensemble. *Climatic Change, Springer Science and Business Media LLC, 114*, 813-822. doi: 10.1007/s10584-012-0570-x.

Diffenbaugh NS, Pal JS, Trapp RJ, Giorgi F, **2005**. Fine-scale processes regulate the response of extreme events to global climate change. *Proceedings of the National Academy of Sciences, Proceedings of the National Academy of Sciences, 102*, 15774-15778. doi: 10.1073/pnas.0506042102.

D'Ippoliti D, Michelozzi P, Marino C, de'Donato F, Menne B, Katsouyanni K, Kirchmayer U, Analitis A, Medina-Ramón M, Paldy A, Atkinson R, Kovats S, Bisanti L, Schneider A, Lefranc A, Iñiguez C, Perucci CA, **2010**. The impact of heat waves on mortality in 9 European cities: results from the EuroHEAT project. *Environmental Research*. doi: 10.1186/1476-069X-9-37.

Fallmann J, Wagner S, Emeis S, **2015**. High resolution climate projections to assess the future vulnerability of European urban areas to climatological extreme events. *Theoretical and Applied Climatology, Springer Science and Business Media LLC, 127*, 667-683. doi: 10.1007/s00704-015-1658-9.

Feudale and Shukla, **2010**. Influence of sea surface temperature on the European heat wave of 2003 summer. Part I: an observational study. *Climate Dynamics, Springer Science and Business Media LLC, 36*, 1691-1703. doi: 10.1007/s00382-010-0788-0.

Ferranti L & Viterbo P, **2006**. The European Summer of 2003: Sensitivity to Soil Water Initial Conditions. *American Meteorological Society.* doi: 10.1175/JCLI3810.1.

Fink AH, Brücher T, Krüger A, Leckebusch GC, Pinto JG, Ulbrich U, **2004**. The 2003 European summer heatwaves and drought -synoptic diagnosis and impacts. *Weather, Wiley, 59*, 209-216. doi: 10.1256/wea.73.04.

Fischer EM, Oleson KW, Lawrence DM, **2012**. Contrasting urban and rural heat stress responses to climate change. *Geophysical Research Letters, American Geophysical Union (AGU), 39*. doi: 10.1029/2011gl050576.

Fischer EM & Schär C, **2010**. Consistent geographical patterns of changes in high-impact European heatwaves. *Nature Geoscience, Springer Science and Business Media LLC, 3*, 398-403. doi: 10.1038/ngeo866.

Fischer EM, Seneviratne SI, Vidale PL, Lüthi D, Schär C, **2007**. Soil Moisture–Atmosphere Interactions during the 2003 European Summer Heat Wave. *Journal of Climate, American Meteorological Society, 20*, 5081-5099. doi: 10.1175/jcli4288.1.

Giorgi F, **2006**. Climate change hot-spots. *Geophysical Research Letters, American Geophysical Union (AGU), 33.* doi: 10.1029/2006gl025734.

Hamdi R, Duchêne F, Berckmans J, Delcloo A, Vanpoucke C, Termonia P, **2016**. Evolution of urban heat wave intensity for the Brussels Capital Region in the ARPEGE-Climat A1B scenario. *Elsevier BV, 17,* 176-195. doi: 10.1016/j.uclim.2016.08.001.

Hamdi R, de Vyver HV, Troch RD, Termonia P, **2013**. Assessment of three dynamical urban climate downscaling methods: Brussels's future urban heat island under an A1B emission scenario. *International Journal of Climatology, Wiley, 34,* 978-999. doi: 10.1002/joc.3734.

Hewitt CD & Lowe JA, **2018**. Toward a European Climate Prediction System. *Bulletin of the American Meteorological Society, American Meteorological Society, 99*, 1997-2001. doi: 10.1175/bams-d-18-0022.1.

IPCC, **2022**: Climate Change 2022: Impacts, Adaptation and Vulnerability. Contribution of Working Group II to the Sixth Assessment Report of the Intergovernmental Panel on Climate Change [H-O Pörtner, DC Roberts, M Tignor, ES Poloczanska, K Mintenbeck, A Alegría, M Craig, S Langsdorf, S Löschke, V Möller, A Okem, B Rama (eds)]. Cambridge University Press. *Cambridge University Press*, Cambridge, UK and New York, NY, USA, 3056 pp. doi:10.1017/9781009325844.

IPCC, **2014**: Climate Change 2014: Impacts, Adaptation, and Vulnerability. Part A: Global and Sectoral Aspects. Contribution of Working Group II to the Fifth Assessment Report of the Intergovernmental Panel on Climate Change [Field, CB, VR Barros, DJ Dokken, KJ Mach, MD Mastrandrea, TE Bilir, M Chatterjee, KL Ebi, YO Estrada, RC Genova, B Girma, ES Kissel, AN Levy, S MacCracken, PR Mastrandrea, and LL White (eds)]. *Cambridge University Press*, Cambridge, United Kingdom and New York, NY, USA, 1132 pp. ISBN 978-92-9169-143-2.

Joly D, Brossard T, Cardot H, Cavailhes J, Hilal M, & Wavresky P, **2010**. Les types de climats en France, une construction spatiale. *Cybergeo, OpenEdition.* doi: 10.4000/cybergeo.23155.

Keat WJ, Kendon EJ, Bohnenstengel SI, **2021**. Climate change over UK cities: the urban influence on extreme temperatures in the UK climate projections. *Climate Dynamics, Springer Science and Business Media LLC, 57*, 3583-3597. doi: 10.1007/s00382-021-05883-w.

Kendon EJ, Prein AF, Senior CA, Stirling A, **2021.** Challenges and outlook for convection-permitting climate modelling. *The Royal Society, 379*, 20190547. doi: 10.1098/rsta.2019.0547.

Kong J, Zhao Y, Carmeliet J, Lei C, **2021**. Urban Heat Island and Its Interaction with Heatwaves: A Review of Studies on Mesoscale. *Sustainability, MDPI AG, 13*, 10923. doi: 10.3390/su131910923.

Laaidi K, Zeghnoun A, Dousset B, Bretin P, Vandentorren S, Giraudet E, Beaudeau P, **2012**. The Impact of Heat Islands on Mortality in Paris during the August 2003 Heat Wave. *Environmental Health Perspectives, Environmental Health Perspectives, 120*, 254-259. doi: 10.1289/ehp.1103532.

Lemonsu A, Caillaud C, Alias A, Riette S, Seity Y, Le Roy B, Michau Y, Lucas-Picher P, **2023**. What added value of CNRM-AROME convection-permitting regional climate model compared to CNRM-ALADIN regional climate model for urban climate studies ? Evaluation over Paris area (France). *Clim Dyn.* doi: 10.1007/s00382-022-06647-w.

Lemonsu A, Beaulant A, Somot S, Masson V, **2014**. Evolution of heat wave occurrence over the Paris basin (France) in the 21st century. *Climate Research, Inter-Research Science Center, 61,* 75-91. doi: 10.3354/cr01235.

Lemonsu A, Kounkou-Arnaud R, Desplat J, Salagnac JL, Masson V, **2013**. Evolution of the Parisian urban climate under a global changing climate. *Climatic Change, Springer Science and Business Media LLC, 116,* 679-692. doi: 10.1007/s10584-012-0521-6.

Lucas-Picher P, Argüeso D, Brisson E, Tramblay Y, Berg P, Lemonsu A, Kotlarski S, Caillaud C, **2021**. Convection-permitting modelling with regional climate models: Latest developments and further steps. *Wiley Interdisciplinary Reviews Climate Change, 12(6), e731*. doi: 10.1002/wcc.731

Lucas-Picher P, Brisson E, Caillaud C, Alias A, Nabat P, Lemonsu A, Poncet N, Hernandez VEC, Michau Y, Doury A, Monteiro D, Somot S, **2023**. Evaluation of the convection-permitting regional climate model CNRM-AROME41t1 over northwestern Europe. *Clim Dyn.* doi: 10.1007/s00382-022-06637-y.

Machard A, Inard C, Alessandrini J-M, Pelé C, Ribéron J, **2020**. A Methodology for Assembling Future Weather Files Including Heatwaves for Building Thermal Simulations from the European Coordinated Regional Downscaling Experiment (EURO-CORDEX) Climate Data. *Energies, MDPI AG, 13*, 3424. doi: 10.3390/en13133424.

Masson V, Moigne PL, Martin E, Faroux S, Alias A, Alkama R, Belamari S, Barbu A, Boone A, Bouyssel F, Brousseau P, Brun E, Calvet J-C, Carrer D, Decharme B, Delire C, Donier S, Essaouini K, Gibelin A-L, Giordani H, Habets F, Jidane M, Kerdraon G, Kourzeneva E, Lafaysse M, Lafont S, Brossier CL, Lemonsu A, Mahfouf J-F, Marguinaud P, Mokhtari M, Morin S, Pigeon G, Salgado R, Seity Y, Taillefer F, Tanguy G, Tulet P, Vincendon B, Vionnet V, Voldoire A, **2013**. The SURFEXv7.2 land and ocean surface platform for coupled or offline simulation of earth surface variables and fluxes. *Geoscientific Model Development, Copernicus GmbH, 6*, 929-960. doi: 10.5194/gmd-6-929-2013.

Masson V, Champeaux J-L, Chauvin F, Meriguet C, Lacaze R, **2003**. A Global Database of Land Surface Parameters at 1-km Resolution in Meteorological and Climate Models. *Journal of Climate, American Meteorological Society, 16*, 1261-1282. doi: 10.1175/1520-0442(2003)16<1261:agdols>2.0.co;2.

Masson V, **2000**. A Physically-Based Scheme For The Urban Energy Budget In Atmospheric Models. *Boundary-Layer Meteorology, Springer Science and Business Media LLC, 94*, 357-397. doi: 10.1023/a:1002463829265.

McCarthy MP, Harpham C, Goodess CM, Jones PD, **2012**. Simulating climate change in UK cities using a regional climate model, HadRM3. *International Journal of Climatology, Wiley, 32*, 1875-1888. doi: 10.1002/joc.2402.

McCarthy MP, Best MJ, Betts RA, **2010**. Climate change in cities due to global warming and urban effects. *Geophysical Research Letters, American Geophysical Union (AGU), 37*. doi: 10.1029/2010gl042845.

Michau Y, Lemonsu A, Lucas-Picher P, Caillaud C, **2023**. Evaluation of the Urban Heat Island of 12 cities of France in a high-resolution regional climate model simulation. *Urban Climate, Elsevier BV, 47*, 101386. doi: 10.1016/j.uclim.2022.101386.

Miralles DG, Teuling AJ, van Heerwaarden CC, de Arellano JVG, **2014**. Mega-heatwave temperatures due to combined soil desiccation and atmospheric heat accumulation. *Nature Geoscience, Springer Science and Business Media LLC, 7*, 345-349. doi: 10.1038/ngeo2141.

Mueller B & Seneviratne SI, **2012**. Hot days induced by precipitation deficits at the global scale. *Proceedings of the National Academy of Sciences, Proceedings of the National Academy of Sciences, 109*, 12398-12403. doi: 10.1073/pnas.1204330109.

Nabat P, Somot S, Cassou C, Mallet M, Michou M, Bouniol D, Decharme B, Drugé T, Roehrig R, Saint-Martin D, **2020**. Modulation of radiative aerosols effects by atmospheric circulation over the Euro-Mediterranean region. *Atmospheric Chemistry and Physics, Copernicus GmbH, 20*, 8315-8349. doi: 10.5194/acp-20-8315-2020.

Oleson KW, **2012**. Contrasts between Urban and Rural Climate in CCSM4 CMIP5 Climate Change Scenarios. *Journal of Climate, American Meteorological Society, 25*, 1390-1412. doi: 10.1175/jcli-d-11-00098.1.

Oleson KW, Bonan GB, Feddema J, Jackson T, **2010**. An examination of urban heat island characteristics in a global climate model. *International Journal of Climatology, Wiley, 31*, 1848-1865. doi: 10.1002/joc.2201.

Ouzeau G, Soubeyroux J-M, Schneider M, Vautard R, Planton S, **2016**. Heat waves analysis over France in present and future climate: Application of a new method on the EURO-CORDEX ensemble. *Climate Services, Elsevier BV, 4*, 1-12. doi: 10.1016/j.cliser.2016.09.002.

Perkins-Kirkpatrick SE & Lewis SC, **2020**. Increasing trends in regional heatwaves. *Nature Communications, Springer Science and Business Media LLC, 11*. doi: 10.1038/s41467-020-16970-7.

Perkins SE & Alexander LV, **2013**. On the Measurement of Heat Waves. *Journal of Climate, American Meteorological Society, 26*, 4500-4517. doi: 10.1175/jcli-d-12-00383.1.

Qasmi S, Sanchez-Gomez E, Ruprich-Robert Y, Boé J, Cassou C, **2021**. Modulation of the Occurrence of Heatwaves over the Euro-Mediterranean Region by the Intensity of the Atlantic Multidecadal Variability. *Journal of Climate, American Meteorological Society, 34*, 1099-1114. doi: 10.1175/jcli-d-19-0982.1.

Robine J-M, Cheung SLK, Roy SL, Oyen HV, Griffiths C, Michel J-P, Herrmann FR, **2008**. Death toll exceeded 70,000 in Europe during the summer of 2003. *Comptes Rendus Biologies, Elsevier BV, 331*, 171-178. doi: 10.1016/j.crvi.2007.12.001.

Russo S, Sillmann J, Fischer EM, **2015**. Top ten European heatwaves since 1950 and their occurrence in the coming decades. *Environmental Research Letters, IOP Publishing, 10*, 124003. doi:10.1088/1748-9326/10/12/124003.

Russo S, Dosio A, Graversen RG, Sillmann J, Carrao H, Dunbar MB, Singleton A, Montagna P, Barbola P, Vogt JV, **2014**. Magnitude of extreme heat waves in present climate and their projection in a warming world. *Journal of Geophysical Research: Atmospheres, American Geophysical Union (AGU), 119*. doi: 10.1002/2014jd022098.

Schär C, Vidale PL, Lüthi D, Frei C, Häberli C, Liniger MA, Appenzeller C, **2004**. The role of increasing temperature variability in European summer heatwave. *Nature, Springer Science and Business Media LLC, 427*, 332-336. doi: 10.1038/nature02300.

Schoetter R, Cattiaux J, Douville H, **2015**. Changes of western European heat wave characteristics projected by the CMIP5 ensemble. *Climate Dynamics, Springer Science and Business Media LLC, 45*, 1601-1616. doi: 10.1007/s00382-014-2434-8.

Schubert SD, Stewart RE, Wang H, Barlow M, Berbery EH, Cai W, Hoerling MP, Kanikicharla KK, Koster RD, Lyon B, Mariotti A, Mechoso CR, Müller OV, Rodriguez-Fonseca B, Seager R, Seneviratne SI, Zhang L, Zhou T, **2016.** Global Meteorological Drought: A Synthesis of Current Understanding with a Focus on SST Drivers of Precipitation Deficits. *Journal of Climate, American Meteorological Society, 29*, 3989-4019. doi: 10.1175/jcli-d-15-0452.1.

Stott P, Stone D, Allen M, **2004**. Human contribution to the European heatwave of 2003. *Nature* 432, 610–614. https://doi.org/10.1038/nature03089

Seity Y, Brousseau P, Malardel S, Hello G, Bénard P, Bouttier F, Lac C, Masson V, **2011**. The AROME-France Convective-Scale Operational Model. *Monthly Weather Review, American Meteorological Society, 139*, 976-991. doi: 10.1175/2010mwr3425.1.

Seneviratne SI, Corti T, Davin EL, Hirschi M, Jaeger EB, Lehner I, Orlowsky B, Teuling AJ, **2010**. Investigating soil moisture–climate interactions in a changing climate: A review. *Earth-Science Reviews, Elsevier BV, 99*, 125-161. doi: 10.1016/j.earscirev.2010.02.004.

Shu C, Gaur A, Wang LL, Bartko M, Laouadi A, Ji L, Lacasse M, **2021**. Added value of convection permitting climate modelling in urban overheating assessments. *Building and Environment, Elsevier BV, 207*, 108415. doi: 10.1016/j.buildenv.2021.108415.

Soares PMM, Careto JAM, Cardoso RM, Goergen K, Katragkou E, Sobolowski S, Coppola E, Ban N, Belušić D, Berthou S, Caillaud C, Dobler A, Hodnebrog Ø, Kartsios S, Lenderink G, Lorenz T, Milovac J, Feldmann H, Pichelli E, Truhetz H, Demory ME, de Vries H, Warrach-Sagi K, Keuler K, Raffa M, Tölle M, Sieck K, Bastin S, **2022**. The added value of km-scale simulations to describe temperature over complex orography: the CORDEX FPS-Convection multi-model ensemble runs over the Alps. *Climate Dynamics, Springer Science and Business Media LLC.* doi: 10.1007/s00382-022-06593-7**.**

Soubeyroux JM, Ouzeau G, Schneider M, Cabanes O, Kounkou R, **2016**. Les vagues de chaleur en France : analyse de l'été 2015 et évolutions attendues en climat futur. *La Météorologie, 94*, 45-51. doi: 10.4267/2042/60704.

Suli S, Barriopedro D, García–Herrera G, Rusticucci M, **2023**. Regionalisation of heat waves in southern South America, *Weather and Climate Extremes, 40*, (100569). doi: 10.1016/j.wace.2023.100569.

Tan J, Zheng Y, Tang X, Guo C, Li L, Song G, Zhen X, Yuan D, Kalkstein AJ, Li F, Chen H, **2009**. The urban heat island and its impact on heat waves and human health in Shanghai. *International Journal of Biometeorology, Springer Science and Business Media LLC, 54*, 75-84. doi: 10.1007/s00484-009-0256-x.

United Nations, Department of Economic and Social Affairs, Population Division, **2019**. World Urbanization Prospects: The 2018 Revision (ST/ESA/SER.A/420). New York: United Nations. ISBN: 978-92-1-148319-2.

Viguié V, Lemonsu A, Hallegatte S, Beaulant A-L, Marchadier C, Masson V, Pigeon G, Salagnac J-L, **2020**. Early adaptation to heat waves and future reduction of air-conditioning energy use in Paris. *Environmental Research Letters, IOP Publishing, 15*, 075006. doi: 10.1088/1748-9326/ab6a24.

Voldoire A, Sanchez-Gomez E, Salas y Mélia D, Decharme B, Cassou C, Sénési S, Valcke S, Beau I, Alias A, Chevallier M, Déqué M, Deshayes J, Douville H, Fernandez E, Madec G, Maisonnave E, Moine M-P, Planton S, Saint-Martin D, Szopa S, Tyteca S, Alkama R, Belamari S, Braun A, Coquart L, Chauvin F, **2012**. The CNRM-CM5.1 global climate model: description and basic evaluation. *Climate Dynamics, Springer Science and Business Media LLC, 40*, 2091-2121. doi: 10.1007/s00382-011-1259-y.

World Meteorological Organization. WMO has no immediate plans to name heatwaves, https://public.wmo.int/en/media/news/wmo-has-no-immediate-plans-name-heatwaves (19/07/2022)

Zampieri M, D'Andrea F, Vautard R, Ciais P, de Noblet-Ducoudré N, Yiou P, **2009**. Hot European Summers and the Role of Soil Moisture in the Propagation of Mediterranean Drought. *Journal of Climate, American Meteorological Society, 22*, 4747-4758. doi: 10.1175/2009jcli2568.1.